



1 Freshening of the Labrador Sea as a trigger for Little Ice Age development

2

3 Montserrat Alonso-Garcia^{1,2,3}, Helga F. Kleiven⁴, Jerry F. McManus⁵, Paola Moffa-Sanchez⁶,

4 Wallace Broecker⁵ and Benjamin P. Flower¹

5

6 1 College of Marine Science, University of South Florida, St. Petersburg, FL, US.

7 2 Instituto Português do Mar e da Atmosfera (IPMA), Div. de Geologia e Georecursos Marinhos,

8 Lisboa, Portugal.

9 3 Centro de Ciencias do Mar (CCMAR), Universidade do Algarve, Faro, Portugal

10 4 University of Bergen and Bjerknes Centre for Climate Research, Postboks 7803, 5020 Bergen,

11 Norway.

12 5 Department of Earth and Environmental Sciences, Lamont-Doherty Earth Observatory of

13 Columbia University, Palisades, NY 10964-8000 USA.

14 6 Department of Marine and Coastal Sciences, Rutgers University, New Brunswick, NJ, 08901,

15 USA.

16 *Correspondence to:* Montserrat Alonso-Garcia (montserrat.alonso@ipma.pt)

17

18 Abstract

19 Arctic freshwater discharges to the Labrador Sea from melting glaciers and sea-ice can have a deep
20 impact on ocean circulation dynamics in the North Atlantic modifying climate and deep water
21 formation in this region. In this study, we present for the first time a high resolution record of ice-
22 rafting in the Labrador Sea over the last millennium to assess the effects of freshwater discharges in
23 this region on ocean circulation and climate. The occurrence of ice-rafted debris (IRD) in the
24 Labrador Sea was studied using sediments from Site GS06-144-03 (57.29° N, 48.37° W, 3432 m
25 water depth). IRD from the fraction 63-150 µm show higher concentration during the intervals:
26 ~1000-1100, ~1150-1250, ~1400-1450, ~1650-1700 and ~1750-1800 yr AD. The first two intervals
27 occurred during the Medieval Climate Anomaly (MCA), whereas the others took place within the
28 Little Ice Age (LIA). Mineralogical identification indicates that the main IRD source during the
29 MCA was SE Greenland. In contrast, the concentration and relative abundance of hematite-stained
30 grains (HSG) reflects an increase in the contribution of Arctic ice during the LIA.



31 The comparison of our Labrador Sea IRD records with other climate proxies from the subpolar
32 North Atlantic allowed us to propose a sequence of processes that led to the cooling events during
33 the LIA, particularly in the Northern Hemisphere. This study reveals that the warm climate of the
34 MCA may have enhanced iceberg calving along the SE Greenland coast and, as a result, freshened
35 the subpolar gyre (SPG). Consequently, SPG circulation switched to a weaker mode through
36 internal feedbacks that reduced convection in the Labrador Sea decreasing its contribution to the
37 Atlantic Meridional overturning circulation and, thus, the amount of heat transported to high
38 latitudes. This mechanism very likely preconditioned the North Atlantic inducing a state in which
39 external forcings (e.g. solar irradiance and volcanic input) could easily drive periods of severe cold
40 conditions in Europe and the North Atlantic like the LIA. The outcomes of this work indicate that a
41 freshening of the SPG may play a crucial role in the development of cold events during the
42 Holocene, which may be of key importance for predictions about future climate.

43

44 Key words: Little Ice Age, Medieval Climate anomaly, Labrador Sea, ice-rafting

45

46 1. Introduction

47 The last millennium is a primary target in paleoclimate studies since this interval allows us to
48 reconstruct the climate variability of our recent history and its impact on the development of our
49 society. Moreover, climatic reconstructions of the last millennium combined with instrumental
50 records constitute a remarkable framework to obtain a comprehensive understanding of the
51 mechanisms that drive the Earth's climate and improve future climate predictions. The climate of
52 the last millennium is characterized by a warm period called the Medieval Climate Anomaly
53 (MCA) or Medieval Warm Period (~800-1200 yr AD), a cold interval called the Little Ice Age
54 (LIA, ~1350-1850 yr AD) and the 20th century warming trend (e.g. Mann et al., 2009; Wanner et
55 al., 2011). According to historical records, these climate oscillations affected human development in
56 Europe, in particular, the Norse expansion in the North Atlantic (Ogilvie et al., 2000). The warm
57 conditions of the MCA promoted the colonization of Iceland and Greenland by the Norse and the
58 exploration of North America during the 9th to 12th centuries, whereas the deterioration of climatic
59 conditions at the beginning of the LIA forced them to abandon the Greenland settlements by the end
60 of the 15th century (Kuijpers et al., 2014; Ogilvie et al., 2000).

61 Reconstructions of ocean and land temperature show the LIA cooling was neither spatially nor
62 temporally uniform (Bradley et al., 2003; PAGES 2k Consortium, 2013; Wanner et al., 2015;



63 Wanner et al., 2011) and, therefore, there is an open debate on the forcings that may have triggered
64 these climate oscillations. Reduced solar irradiance and the occurrence of explosive volcanic
65 eruptions are the two most commonly examined forcings (e.g. Bond et al., 2001; Miller et al., 2012)
66 due to the impact they may have on atmospheric dynamics. Other forcings such as the internal
67 dynamics of the oceanic and atmospheric systems (such as the North Atlantic Oscillation-NAO-,
68 Arctic Oscillation-AO-, Atlantic Multidecadal Oscillation-AMO-, El Niño-Southern Oscillation-
69 ENSO-, or the monsoonal regimes) have also been considered to play a major role driving climate
70 oscillations during the last century (see review in Wanner et al., 2011). Freshwater discharges to the
71 North Atlantic may also be the drivers of climate change through their impact on sea surface
72 circulation and deep water convection, which in turn may slowdown the Atlantic Meridional
73 Overturning Circulation (AMOC) (Manabe and Stouffer, 1995). Particularly, the Labrador Sea is
74 very sensitive to increases in freshwater and sea ice input. Deep water formation in the Labrador
75 Sea contributes 30% of the volume transport of the deep limb of the AMOC (Rhein et al., 2002;
76 Talley, 2003), and freshwater input to this region reduces deep convection and deep water
77 formation, slowing down the overturning circulation and oceanic heat transport by up to 27 and 15
78 %, respectively (Born et al., 2010). The decrease in heat export from low to high latitudes modifies
79 regional climate by cooling the western North Atlantic which, in turn, influences the climate of the
80 whole North Atlantic (Born et al., 2010). A recent example of this phenomenon may be the Great
81 Salinity Anomaly (Dickson et al., 1988). During this event, vast amounts of Arctic sea ice and
82 freshwater were delivered to the Labrador Sea, mainly via the East Greenland Current (EGC),
83 freshening the subpolar gyre (SPG) and decreasing winter convection and deep water production. A
84 recent study of the last 50 years also shows a close relationship between fresh water fluxes from the
85 Arctic and reductions in deep water formation in the Labrador Sea (Yang et al., 2016).

86 Recently, a lot of attention has been paid to the dynamics of the SPG and its relationship with
87 climate (e.g. Born and Stocker, 2014). Instrumental records and modern observations show a close
88 link between decadal climate variability and SPG dynamics (e.g. Hakkinen and Rhines, 2004;
89 Sarafanov, 2009), and rapid climate change reconstructions throughout the last glacial cycle have
90 been interpreted as a consequence of changes in the SPG dynamics (Moffa-Sanchez et al., 2014a;
91 Mokeddem and McManus, 2016; Mokeddem et al., 2014; Moros et al., 2012; Thornalley et al.,
92 2009). Variations in the strength and shape of the SPG may also impact deep convection in the
93 Labrador Sea, therefore influencing deep water production and AMOC (Böning et al., 2006; Hatun
94 et al., 2005), which eventually affects climate through the reduction of heat transported from low to
95 high latitudes. A shift to weak SPG circulation has been inferred using deep-sea corals between the
96 MCA and the LIA (Copard et al., 2012) and model simulations suggested this weakening of the



97 SPG was the main driver of the LIA due to the decrease in meridional heat transport to the subpolar
98 North Atlantic (Moreno-Chamarro et al., 2016). Moreover, the occurrence of unusually cold winters
99 in Europe during the last 100 years has been associated with atmospheric blocking events in the
100 North Atlantic, which are high pressure systems that alter the normal westerly wind circulation in
101 this region (Häkkinen et al., 2011). These events are associated with negative NAO, may modify
102 surface circulation in the North Atlantic and are linked to cold winter temperature in western
103 Europe (Shabbar et al., 2001). Periods of intense and persistent atmospheric blocking events very
104 likely developed during the LIA due to the influence of low solar irradiance and weak SPG
105 circulation, causing decadal intervals of severe cooling in Europe (Moffa-Sanchez et al., 2014a).

106 In this work we used a sediment core from the Eirik Drift, in the Labrador Sea, to reconstruct the
107 ice-rafting occurrence during the last 1200 yr and examine its impact on SPG dynamics and climate.
108 The presence of ice-rafted debris (IRD) is a proxy for iceberg and sea ice discharges. Our IRD
109 record from the Eirik Drift indicates ice export to the Labrador Sea and allows us to infer periods of
110 enhanced freshwater discharges. Previous Holocene multi-proxy records (including IRD records)
111 from the North Atlantic pointed to the linkage between cooling events and low solar irradiance
112 values (Bond et al., 2001). However, this hypothesis has been challenged by the fact that ice-rafting
113 reconstructions in the Northern North Atlantic show different trends between the eastern and
114 western regions during the Holocene (Moros et al., 2006). The combination of our IRD data with
115 other records from Eirik Drift as well as other subpolar North Atlantic sites allowed us to present a
116 comprehensive reconstruction of the transition from the MCA to the LIA. This study reveals the
117 importance of ice discharges in modifying surface circulation in the SPG, as a driver of oscillations
118 in climatic patterns and deep water production in the past, and perhaps again in the near future.

119

120 2. Geological and oceanographic setting

121 Site GS06-144-03 (57.29° N, 48.37° W, 3432 m water depth) is located in the southern tip of
122 Greenland at the Eirik drift (Fig. 1). The site is placed in the northwest part of the SPG, a very
123 sensitive area to climatic and oceanographic changes given that the upper North Atlantic deep water
124 forms in this region (Schmitz and McCartney, 1993). The SPG boundary currents are formed by the
125 North Atlantic current (NAC), the Irminger current (IC), which is the western branch of the NAC
126 and flows towards Greenland, the East Greenland current (EGC) and the Labrador Current (LC)
127 (Fig.1). The IC brings warm and high salinity water to the Labrador Sea whereas the EGC and LC
128 transport colder and lower salinity water and usually carry icebergs and sea ice from the Arctic area.



129 Oscillations in the amount of ice transported by the EGC and LC may result in freshening of the
130 SPG affecting the strength of SPG circulation. Fluctuations in the SPG circulation have been
131 suggested as the driver of oscillations in decadal deep water production and climate variability in
132 the North Atlantic and surrounding continents (Böning et al., 2006; Hakkinen and Rhines, 2004;
133 Hatun et al., 2005). Two states of equilibrium have been described depending on the strength of the
134 SPG circulation (Born and Stocker, 2014), when the circulation is strong, more salty water is
135 advected to the center of the gyre favouring deep water formation in this area, whereas when the
136 circulation is weak more salty water is advected northeastward to the Nordic Seas and the SPG
137 water gets fresher, which prevents deep convection in the Labrador Sea. However, some increased
138 convection may occur in the Irminger Basin and Nordic Seas, counterbalancing the lack of
139 Labrador Sea convection. Changes in the dynamics of the SPG are mainly driven by cyclonic winds
140 and buoyancy forcing (Born and Stocker, 2014), therefore, freshwater input via iceberg discharges
141 may be a critical factor modifying the circulation in the SPG and the deep water formation in the
142 Labrador Sea.

143

144 3. Materials and methods

145 Sediments from Site GS06-144-03 were drilled using a multicore device during a cruise on the R/V
146 G.O. Sars (Dokken and Ninnemann, 2006). A robust chronology has been developed based on 12
147 AMS radiocarbon dates and ^{210}Pb measurements at the top of the core (Kleiven et al. in prep.).
148 Samples were taken every 0.5 cm and the high sedimentation rate at this site allows us to
149 reconstruct the ice-rafting history of the past 1200 yr at a decadal-scale resolution (mean
150 sedimentation rate of 0.029 cm/yr, on average ~17 yr between samples). Sediment samples were
151 sieved using a 63 μm mesh with de-ionized water to eliminate clays and subsequently dried in an
152 oven. Then samples were dry sieved to extract 63-150 μm fraction which was used in this study to
153 examine IRD content. This size fraction is coarse enough to be delivered to the open ocean
154 primarily by drifting ice rather than wind or currents (Fillon et al., 1981; Ruddiman, 1977), yet
155 lends itself to detailed petrographic analysis (Bond and Lotti, 1995).

156 Each sample was split with a microsplitter to obtain an aliquot with about 200 IRD grains. The
157 aliquots were placed in a transparent gridded tray and counted using a high magnification
158 stereomicroscope which incorporates a light source from the bottom, similar to the transmitted light,
159 and a light source from the top which emulates reflected light. Using aliquots in a transparent tray
160 instead of smear slides offers the possibility of moving the grains independently, thus allowing for a
161 better identification. Additionally, the use of a transparent tray is a key factor to improve the



162 identification of quartz and feldspar hematite-stained grains (HSG) by the introduction of a white
163 paper below the tray which enhances the contrast between the hematite-stained portion and the rest
164 of the grain. This technique is similar to that described in Bond et al. (1997), however, the use of
165 aliquots presents the advantage that IRD concentrations in the bulk sediment can be calculated to
166 obtain the total number of IRD (and IRD types) per gram of bulk sediment. A minimum of 200
167 grains were counted in each sample and the calculated errors for the replicated samples are below
168 3.2 %. The identification of different groups of minerals such as HSG of quartz and feldspar,
169 unstained quartz and feldspar, and brown and white volcanic glass (VG) allows us to calculate the
170 relative abundance of each type of IRD which may be useful to identify the sources of the drifting
171 ice that transported the IRD (e.g. Alonso-Garcia et al., 2013; Bailey et al., 2012).

172 SEM x-ray diffraction was performed on selected grains with an energy dispersive spectroscopy
173 (EDS) equipment at the facilities of the College of Marine Science (University of South Florida).
174 The EDS equipment used is an EDAX x-ray microanalysis system with an Apollo 10 silicon drift
175 detector.

176

177 4. Results

178 The total concentration of IRD (Fig. 2) ranges from ~9,000 to 116,000 grains per gram of sediment
179 (grains/g) which means that icebergs and sea ice reached the studied area during the entire interval
180 examined in this work. The highest peak of IRD concentration was reached at the end of the MCA
181 (1169 yr AD) and the intervals with higher IRD concentration occurred approximately at 1000-
182 1100, 1150-1250, 1400-1450, 1650-1700 and 1750-1800 yr AD with mean values above 50,000
183 grains/g. The first two of these five intervals of high ice-rafting occurred during the MCA, whereas
184 the other three intervals of high IRD concentration took place during the LIA.

185 Volcanic glass (VG) is one of the main components of the IRD with relative abundances up to 59 %
186 (Fig. 2). This group includes brown VG fragments, usually not vesicular, and white VG fragments,
187 very light and often with vesicular aspect. The concentration of the total VG shows a similar pattern
188 to the total IRD concentration with higher values during the same intervals (Fig. 2). The relative
189 abundance of VG shows higher values during the intervals of higher total IRD concentration. The
190 relative abundance of white VG is generally lower than 20 % and does not show clear periods of
191 higher abundance that can be correlated to the record of volcanic eruptions (Gao et al., 2008).

192 HSG relative abundance ranges between 2 and 30 %, reaching higher values than those observed at
193 MC52 in the Eastern North Atlantic (Fig. 3, Bond et al., 2001). The record of HSG concentration



194 shows a different pattern from the total IRD and VG records, with higher concentration from 1400
195 to 1900 yr AD (Fig. 2). The relative abundance of HSG is also higher after 1400 yr AD, with mean
196 values increasing to over 15 % from near 5% before 1400 yr AD. This range of variability is
197 comparable to previous observations across the Atlantic in the late Holocene (Bond et al., 1997;
198 2001).

199 Among the selected grains to perform x-ray analysis we separated a group of black unclassified
200 minerals. According to the SEM x-ray diffraction analysis, those grains are mainly composed by
201 carbon, and we interpreted them as coal fragments. Those minerals occurred in higher abundance
202 during the MCA and the end of the LIA.

203

204 5. Discussion

205 5.1. IRD sources and significance

206 The mineralogy found at Site GS06-144-03 suggests several lithological sources for the IRD which
207 may be associated with icebergs or sea-ice originated from different areas. Volcanic rocks outcrop
208 mainly in Iceland and the Geikie Plateau area on the East Greenland coast, surrounding Denmark
209 Strait (Bailey et al., 2012; Henriksen et al., 2009). Volcanic glass can also be atmospherically
210 transported after volcanic eruptions and be ultimately incorporated in the ice as it has been shown in
211 Greenland ice core records (Grönvold et al., 1995). This is very likely the case of the white VG
212 fragments found in our record because our counts of white VG (Fig. 2) do not suggest the presence
213 of any discrete layer that could be associated with any dated Icelandic eruption (Gao et al., 2008).
214 This type of IRD was probably deposited on the top of glaciers and sea-ice near Iceland and the
215 East Greenland coast and then transported in the ice through the EGC. Although some of those
216 volcanic shards ejected to the atmosphere could have fallen directly in the sea, the preferentially
217 eastward dispersal pattern of Icelandic tephra following the predominantly westerly winds in the
218 stratosphere (Lacasse, 2001) argues against the hypothesis of volcanic glass transported by winds to
219 the study site. Moreover, previous studies suggested the significantly low amounts of tephra
220 transported towards Greenland prevent finding layers that can be associated with volcanic eruptions
221 (Jennings et al., 2014). After detailed geochemical studies Jennings et al. (2014) could not recognise
222 any specific layer that could be used as a tephrochronological event in the SE Greenland coast
223 during the last millennium. Brown VG fragments are generally solid and not vesicular, suggesting
224 that they are not windblown shards and were more likely to have been incorporated in the ice from
225 outcrops in Greenland and Iceland. Similar brown VG fragments were described in
226 Kangerdlugssuaq trough sediments and were interpreted as coming from the glaciers and sea ice



227 from the Geikie Plateau area, based on mineralogical and x-ray diffraction analysis data (Alonso-
228 Garcia et al., 2013).

229 The presence of HSG in Eirik Drift sediments indicates drift-ice coming from NE Greenland and
230 the Arctic, where red sandstones outcrop (Bond et al., 1997; Henriksen et al., 2009). Most of the
231 glaciers in NE Greenland and the Arctic develop floating ice tongues in the fjords where semi-
232 permanent fast-ice hinders the icebergs from drifting. As a result, most of the IRD carried at the
233 base of the icebergs is deposited in the fjords (Reeh et al., 2001). Our HSG record from the Eirik
234 Drift shows a significant amount (up to 30%) of this type of IRD. Therefore, despite substantial
235 deposition of debris within the fjords, the remainder of the drifted ice still carries considerable
236 amounts of IRD. We suggest that some of that IRD may have been wind-blown to the top of the
237 glaciers and/or sea ice at the NE Greenland and Arctic coasts and fjords, rather than directly
238 incorporated in the bottom layers of the glacier. Those grains were then ice-rafted southwards by
239 the EGC when the ice was released from the fjords. A similar origin was proposed for HSG
240 deposited at the SE Greenland coast based on a multi-proxy study (Alonso-Garcia et al., 2013). In
241 this study, periods of higher HSG abundance were associated with strong ice export from the Arctic
242 via the EGC.

243 Variations in Arctic ice export show a significantly positive correlation with the wintertime North
244 Atlantic/Arctic Oscillation (NAO/AO) during the last decades (e.g. Dickson et al., 2000), although
245 it also depends on the meridional wind components and the position of the atmospheric pressure
246 centers (Hilmer and Jung, 2000). Indeed, during the “Great Salinity Anomaly” the freshwater and
247 ice input to the subpolar North Atlantic happened during a NAO negative phase (Dickson et al.,
248 2000). Additionally, Darby et al. (2012) demonstrated that the sources of Arctic sea ice may change
249 following the AO and, therefore, we can observe changes in the mineralogy transported by the ice
250 in sediment cores influenced by the EGC. During the negative state of the AO a strong high
251 pressure system dominates the Beaufort Sea restricting the Trans-Polar Drift to the Siberian side of
252 the Arctic Ocean (Mysak, 2001; Rigor et al., 2002) which would bring drift-ice with HSG from the
253 areas of Severnaya Zemlya and Franz Josef Land. The increase in HSG relative abundance and
254 concentration at Eirik Drift after 1400 yr AD (Fig. 3) coincides with the shift from positive to
255 negative NAO conditions reconstructed using tree rings, speleothems and lake records (Olsen et al.,
256 2012; Trouet et al., 2009). This switch in NAO conditions may have intensified Arctic sea ice
257 export at the beginning of the LIA, leading to the observed increase in HSG. The sedimentary
258 record of Feni Drift (Bond et al., 2001), in the NE Atlantic, also shows an increase in HSG relative
259 abundance during the LIA (Fig. 3). Furthermore, another proxy, the sodium (Na⁺) concentration in



260 the Greenland ice core GISP2 (Meeker and Mayewski, 2002) indicates an increase in storminess at
261 ~1400 yr AD. The amount of Na⁺ in Greenland ice cores has been interpreted as controlled by the
262 Icelandic Low, and hence, the increase in Na⁺ may be linked to the NAO negative phase. Enhanced
263 storminess favours the transport of icebergs and sea ice through the EGC as well as the deposition
264 of HSG in the sea ice and on top of glaciers, and both processes increase the amount of HSG
265 transported to Eirik Drift. Greenland temperature also shows a decreasing trend after ~1400 yr AD,
266 coinciding with the shift to predominantly negative NAO (Kobashi et al., 2010). Colder
267 atmospheric temperatures and the increase in ice drifted from the Arctic may have contributed to
268 decrease subpolar sea surface temperature in the subpolar area, favouring icebergs to reach areas
269 further south such as Feni Drift (Bond et al., 2001).

270 Coal bearing sediments are present at many areas around the Arctic such as Siberia, Northern
271 Canada, Greenland and Scandinavia (Polar Region Atlas, 1974; Petersen et al., 2013) and contribute
272 to high-latitude IRD deposition (Bischof and Darby, 1997; McManus et al., 1996). Even though the
273 percentage of coal fragments is rather low at our study site (under 5 %, see Fig. 2) the higher
274 abundance of coal fragments in the Labrador Sea during the MCA may be related to an increase in
275 drift-ice from the Canadian Arctic during the positive state of NAO/AO. However, these fragments
276 might also indicate human-related activity which increased in the area during the MCA. Further
277 analysis should be performed to assess the linkage of those grains to any specific source.

278 Regardless of the mineralogy of the grains, it is noteworthy the high number of lithics per gram of
279 sediment recorded in several samples during the MCA (Fig. 2). A recent comprehensive study of
280 the last 2 millennia (PAGES 2k Consortium, 2013) shows this interval presented sustained warm
281 temperatures from 830 to 1100 yr AD in the Northern Hemisphere, including the Arctic region. The
282 high occurrence of IRD from 1000 to 1250 yr AD suggests that during the MCA either a substantial
283 amount of icebergs drifted to the study area or the drifting icebergs contained considerable amounts
284 of IRD, or a combination of both explanations. Several studies on East Greenland glaciers and
285 fjords point to the consistent relationship between calving rate acceleration and the presence of
286 warm Atlantic water in East Greenland fjords, brought by the Irminger current (Andresen et al.,
287 2012; Jennings and Weiner, 1996). Warm atmospheric temperatures as well as the presence of
288 Atlantic water prevent the formation of sea ice in the fjords and in front of the glacier, thus
289 increasing the calving rate by destabilizing the glacier tongue (Andresen et al., 2012; Murray et al.,
290 2010). When tidewater glaciers are released from the sea ice, their speed increases due to the
291 decreased flow-resistance and increased along-flow stresses during the retreat of the ice front, and
292 rapid changes may be observed in calving rates in response to disequilibrium at the front (Joughin et



293 al., 2008). At present, Kangerdlugssuaq and Helheim glaciers, located in the central East Greenland
294 coast, represent the 35 % of East Greenland's total discharge (Rignot and Kanagaratnam, 2006). If
295 conditions during the MCA were similar or warmer than at present, the calving rates of these
296 glaciers may have been even higher than at present, delivering vast amounts of icebergs to the EGC,
297 where they would release IRD as they melted. Moreover, during the MCA it is likely that other
298 fjords, such as Nansen and Scoresby Sund, were also ice free during the summer, allowing them to
299 contribute considerable numbers of icebergs to the EGC. The massive diamicton found in Nansen
300 fjord sediments between 730 and 1100 yr AD demonstrates that there was continuous iceberg
301 rafting due to warmer conditions (Jennings and Weiner, 1996). In this context, we postulate that
302 warm temperatures were the driver of the increased iceberg calving at Greenland fjords and the high
303 accumulation of IRD at Eirik Drift during late MCA.

304 After 1250 yr AD several spikes of high IRD abundance occurred during the intervals 1400-1450 yr
305 AD, 1650-1700 and 1750-1800 yr AD (Fig. 2). Because those intervals occurred within the LIA and
306 under cold conditions the trigger of iceberg production must have been slightly different from the
307 drivers proposed for the MCA ice-rafting events. These intervals of higher IRD accumulation
308 during the LIA are characterized by slightly lower relative abundance of HSG and higher relative
309 abundance of volcanic grains and other fragments. This points to an intensification of SE Greenland
310 production of icebergs during the LIA intervals of enhanced ice-rafting. Therefore, for the LIA
311 events, we advocate for the same mechanism that was put forward to explain rapid releases of
312 icebergs in Denmark Strait during the last 150 yr (Alonso-Garcia et al., 2013). During cold periods
313 sea ice becomes perennial along the Greenland coast blocking the seaward advance of glaciers and
314 hindering icebergs from calving, thus leading to the accumulation of ice mass in the fjords. Based
315 on model simulations, when the sea ice opens or breaks, the ice flow at the grounding line
316 accelerates very quickly, triggering a rapid release of the grounded ice stream (Mugford and
317 Dowdeswell, 2010). In summary, we propose that the high IRD occurrence during the intervals
318 1350-1450 yr AD, 1650-1700 and 1750-1800 yr AD very likely corresponds to episodes of rapid
319 iceberg release from SE Greenland fjords. Interestingly, the timing of these intervals of high IRD
320 deposition coincides with the events of volcanic-solar downturns described by the PAGES 2k
321 Consortium (2013).

322

323 5.2. Influence of ice-rafting on SPG conditions and climate during the last millennium

324 Our IRD records have been compared with other paleoceanographic and paleoclimatic records from
325 Eirik Drift and other subpolar North Atlantic sites to obtain a better picture of subpolar conditions



326 during the last millennium. The planktic foraminifer $\delta^{18}\text{O}$ record of *Globigerina bulloides* and the
327 *Neogloboquadrina pachyderma* sin relative abundance from Eirik Drift (Moffa-Sanchez et al.,
328 2014a; Moffa-Sanchez et al., 2014b) suggest a cooling episode during late MCA (~1100 yr AD) and
329 a clear drop in temperature after 1200 yr AD (Fig. 4). The coincidence of these temperature drops
330 with the increasing trend in total IRD concentration at site GS06-144-03, indicates that the growing
331 iceberg production at East Greenland fjords, due to the MCA warm conditions, started to cool and
332 freshen Labrador Sea several centuries before the LIA started. The quartz/plagioclase ratio, a bulk
333 measure of IRD (Moros et al., 2004), also shows an increasing trend at the end of the MCA at sites
334 in Denmark Strait (Andrews et al., 2009a; see Fig. 4) and off northern Iceland (Moros et al., 2006)
335 providing further evidence for the intensification of iceberg calving at this time. Colder winter sea
336 surface conditions have also been recorded off N Iceland after 1200 yr AD (Jiang et al., 2007)
337 although the sea ice index indicates the first period of severe sea ice conditions only started at
338 ~1300 yr AD (Massé et al., 2008) when annual SST substantially decreased (Sicre et al., 2008), in
339 agreement with the Denmark Strait data (Fig.4). The reduction in the relative abundance of the
340 benthic foraminifer *Cassidulina teretis* between 1000 and 1300 yr AD in Nansen fjord indicates a
341 weaker influence of Atlantic water at the East Greenland coast (Jennings and Weiner, 1996). This
342 decline in Atlantic water may be explained by a weakening in the northern branch of the Irminger
343 current which would have favoured the SST decrease and sea ice formation in Denmark Strait and
344 North of Iceland (Blindheim and Malmberg, 2005). These authors associated the northern Irminger
345 current weakening with high pressure over Greenland and northerly winds. Moreover, other proxies
346 from Denmark Strait indicate the strengthening of N and NW winds after ~1250 yr AD, which led
347 to progressive presence of sea ice exported from the Arctic during winter and spring (Andrews et
348 al., 2009a; Andrews et al., 2009b).

349 The remarkably high Atlantic temperatures recorded during the interval ~950-1100 yr AD (Mann et
350 al., 2009) may indicate SPG circulation was in the strong mode during that time interval (Fig. 4 &
351 5). Strong SPG circulation enhances the supply of warm Atlantic Intermediate water to the East
352 Greenland coast, which promotes calving and, subsequently, increases the ice input in the Labrador
353 Sea region. Switches from weak to strong SPG circulation may happen naturally due to external or
354 internal forcings, and these changes are currently a matter of debate because of their influence on
355 North Atlantic climate (e.g. Hakkinen and Rhines, 2004). According to model simulations,
356 freshwater input (i.e. ice input) to the SPG may trigger weakening of SPG circulation, and this may
357 be amplified successively by positive feedbacks resulting in further weakening and freshening of
358 the gyre due to the attenuation of the Irminger current (Born et al., 2010). Specifically for this time
359 interval, it is important that the main freshwater source was in SE Greenland and reached directly



360 the Labrador Sea, because a freshwater input into the Nordic Seas may have driven the opposite
361 effect (Born and Stocker, 2014). Our IRD record evidences an increase in the amount of ice
362 transported by the EGC to the Labrador Sea from 1000 to 1250 yr AD. This input of freshwater to
363 the SPG potentially drove a slowdown of deep convection in this area and weakened the SPG
364 circulation. A recent study also points to enhanced input of the Labrador current to the Labrador
365 Sea from ~1000 to 1300 yr AD (Sicre et al., 2014), which indicates calving intensified in SW
366 Greenland and Baffin Bay regions as well. Probably ice from both sources, East and West
367 Greenland, directly affected the salinity balance of Labrador Sea water and deep convection in this
368 region. However, even though the freshwater input started at ~1000 yr AD, the SPG circulation
369 only started to weaken after ~1250 yr AD, as suggested by a record of deep-sea corals from the NE
370 Atlantic (Copard et al., 2012). Moreover, our IRD data shows a lag between the first temperature
371 drops at Eirik Drift and the decrease in ice-rafting (Fig. 4), indicating a possible hysteresis between
372 SPG weakening and Irminger current slowdown. It seems the SPG entered in the weak mode,
373 because of the reduced convection, but warm intermediate water remained in the fjords for several
374 years, allowing continued iceberg calving. Also, the response of calving may be slower, particularly
375 if SST were relatively warm and the fjords were not perennially covered by sea ice.

376 As the strength of Irminger current input declined, the areas of Denmark Strait and North of Iceland
377 cooled, and coastal sea ice became perennial after 1450 yr AD, according to the sea ice index IP_{25}
378 (Massé et al., 2008). The *Turborotalita quinqueloba* $\delta^{18}O$ record from Eirik Drift (Moffa-Sanchez et
379 al., 2014b) indicates a shift to colder summer SST in the SPG after 1400 yr AD (Fig. 4), which
380 coincides with the increase in Arctic ice export reflected by the HSG, the storminess intensification
381 (Fig. 3), recorded by the Na^+ content in the Greenland ice core GISP (Meeker and Mayewski,
382 2002), and the shift to negative NAO conditions (Trouet et al., 2009). Planktic $\delta^{18}O$ and Mg/Ca
383 from sites in the Norwegian Sea display an initial decrease in temperature at 1200 yr AD and a
384 subsequent distinct downward shift at ~1400 yr AD, which suggests not only SST cooling but also a
385 decline in the stratification of the water column, very likely linked to changes in atmospheric
386 conditions (Nyland et al., 2006; Sejrup et al., 2010). It is clear that sea surface conditions in the
387 subpolar gyre were rather different before and after ~1200 yr AD. The freshening of the SPG and
388 the increase in sea ice along the Greenland and Iceland coasts may have been associated with a
389 change in atmospheric conditions, deepening the Icelandic Low and intensifying winter circulation
390 over the North Atlantic, i.e. promoting NAO negative conditions and storminess in the subpolar
391 area. Model simulations point to the development of frequent and persistent atmospheric blocking
392 events, induced by low solar irradiance, as one of the main drivers to develop the consecutive cold
393 winters documented in Europe during the LIA (Moffa-Sanchez et al., 2014a). Atmospheric blocking



394 events derive from instabilities of the jet stream which divert or block the pathway of the westerly
395 winds (Häkkinen et al., 2011). These events typically predominate during winter and occur linked
396 to negative NAO index. The cold SST recorded at the subpolar area during low solar irradiance
397 periods (Moffa-Sanchez et al., 2014a; Moffa-Sanchez et al., 2014b; Sejrup et al., 2010), suggest that
398 atmospheric blocking events affected the entire North Atlantic regional climate.

399

400 5.3. Implications for LIA origin and Norse colonies

401 It is worth noting that our IRD record shows two types of ice-rafting events: ice-rafting related to
402 warm temperatures (during the MCA), and ice-rafting linked to rapid releases of the ice
403 accumulated in the fjords due to cold conditions (during the LIA). During the LIA, the events of
404 maximum ice-rafting are closely coupled with the minimum values of solar irradiance (Steinhilber
405 et al., 2009), particularly with the Wolf, Spörer and Maunder minima (Fig. 5). The reconstruction of
406 radiative forcing based on solar irradiance and volcanic eruptions (Crowley, 2000) also shows low
407 values during the main events of high IRD occurrence (Fig. 5). Ice-rafting events tend to happen
408 during intervals of low solar irradiance and cold temperatures in the SPG, often with also
409 significantly cold summer SST (Fig. 4). Solar irradiance has been put forward as the main trigger
410 for the Holocene cold events because low solar irradiance induces an atmospheric reorganization
411 which produces a situation similar to the NAO negative phase (e.g. Bond et al., 2001). Several
412 records from the high latitude North Atlantic support this hypothesis, displaying cold temperatures
413 at times of solar irradiance minima during the last millennium (Moffa-Sanchez et al., 2014a; Sejrup
414 et al., 2010). Precisely dated records of ice-cap growth from Arctic Canada and Iceland show that
415 LIA summer cooling and ice growth began abruptly between 1275 and 1300 yr AD, followed by a
416 substantial intensification at 1430-1455 yr AD (Miller et al., 2012). Those authors pointed to the
417 high volcanic activity during this interval as the main driver for the atmospheric reorganization.
418 However, a comprehensive review on the topic proposed that a combination of internal and external
419 forcings contributed to drive Holocene cold events, including the LIA (Wanner et al., 2011), and
420 recent modelling studies indicated that the weakening of the SPG circulation was not related to
421 either solar or volcanic forcing (Moreno-Chamarro et al., 2016).

422 According to our observations, the increase in Greenland calving during the MCA (Fig. 5) took
423 place before the ice caps started to grow, during an interval of high solar irradiance, high
424 temperatures in the Northern Hemisphere, and low volcanic forcing. This indicates that the ice-
425 rafting events of the MCA were not related to the fluctuations driven by solar-volcanic forcing.
426 Alternatively, we interpret these events as resulting from the acceleration of calving rates in SE



427 Greenland glaciers, driven by warm temperatures. We postulate that the increase in calving rates
428 during the MCA induced a decrease in the Labrador Sea salinity, which may have triggered the
429 weakening of SPG circulation and reduced convection. A decline in Labrador Sea convection
430 reduces deep water formation in one of the key areas of the North Atlantic, which weakens the
431 AMOC, and in turn decreases oceanic heat transport to this area (Born et al., 2010; Moreno-
432 Chamarro et al., 2016). Once the SPG entered in the weak mode this area received less heat and
433 became more sensitive to external forcings which may have generated further cooling. This
434 interpretation is in agreement with recent model simulations which suggest that a weakening of the
435 SPG circulation could have induced the LIA cooling, and this shift from strong to weak circulation
436 may have been triggered by freshwater input to the Labrador Sea (Moreno-Chamarro et al., 2016).
437 Subsequently, low solar irradiance intervals, possibly combined with volcanic emissions, promoted
438 atmospheric reorganizations which gave rise to prevailing negative NAO conditions and/or
439 atmospheric blocking events, enhancing cold temperatures in the subpolar area and promoting ice
440 sheet growth in the Arctic region during the LIA. The development of atmospheric blocking events
441 in the North Atlantic, as suggested by Moffa-Sanchez et al. (2014a), probably propagated the
442 atmospheric cooling across Europe and the Nordic Seas. Indeed, the first strong minimum of solar
443 irradiance associated with the LIA (Wolf, ~1300 yr AD) occurred when the Labrador Sea was
444 already fresher and SPG circulation was weak (Fig. 5), according to our interpretations and to
445 Copard et al. (2012) deep-sea corals record. The reconstruction of combined solar and volcanic
446 forcing (Fig. 5) shows a trend of lower values after 1450 yr AD with a first step of low values
447 during the Wolf minimum indicating that volcanic forcing may also have played an important role
448 in modifying the atmospheric conditions. However, we consider that the decrease in Labrador Sea
449 salinity prior to the Wolf minimum was crucial to produce changes in SPG circulation. Once the
450 SPG entered the weak mode, the effects of solar and volcanic forcing produced a deeper impact on
451 North Atlantic climate. It is likely that the LIA would not have been such a cold and widespread
452 event if the SPG circulation was strong and deep convection was active at the time.

453 The results of this study can be linked to the expansion and demise of the Norse colonies.
454 According to historical data the Norse expansion and colonization of Iceland and Greenland
455 occurred during the warmer climate conditions of the MCA which favoured fishing and farming in
456 these regions (Kuijpers et al., 2014; Ogilvie et al., 2000; Ogilvie and Jónsson, 2001; see Fig. 3). Our
457 study indicates that even though calving intensified after the settlement of the Norse colonies in
458 Greenland, climatic conditions during the late MCA were still favourable because the strong
459 circulation in the SPG supplied relatively warm water to SE Greenland coast. Therefore, the fjords
460 were not perennially covered by sea ice and it is likely that a rather continuous calving may have



461 helped hunting. However, after several decades of intense calving and melting of Greenland
462 glaciers, the Labrador Sea got fresher and the SPG circulation started to weaken triggering a change
463 in oceanic and atmospheric conditions. The reduction of deep convection decreased the transport of
464 heat to the NW subpolar area and enhanced sea ice occurrence in the fjords, which deteriorated the
465 living conditions in Greenland. The subsequent cooling and increase in storminess brought by the
466 shift in atmospheric conditions (predominant NAO negative state and increase in atmospheric
467 blocking events) very likely prompted the abandonment of the Greenland Norse settlements at the
468 beginning of the LIA (Ogilvie et al., 2000, Fig. 3).

469

470 6. Conclusions

471 Sediments from Eirik Drift were studied in order to examine the variations in ice-rafting during the
472 last millennium and its linkage to LIA development. IRD in the 63-150 μm fraction show higher
473 concentration during the intervals: ~1000-1100, ~1150-1250, ~1400-1450, ~1650-1700 and ~1750-
474 1800 yr AD. The identification of different minerals allowed us to link the IRD with potential
475 sources and better interpret the ice-rafting events. The main IRD source was along the SE
476 Greenland coast, although during the LIA the greater concentration and relative abundance HSG
477 supports an increase in the contribution of ice exported from the Arctic region and NE Greenland
478 via the EGC. Two different types of ice-rafting events have been recognised: (1) ice-rafting
479 recorded during the MCA, which we interpret as being related to the acceleration of calving rates in
480 SE Greenland glaciers driven by warm oceanic and atmospheric temperature; and (2) ice rafting
481 events during the LIA, which have been linked to rapid releases of the ice accumulated in the fjords
482 due to the perennial sea ice developed in Greenland coast during cold periods.

483 The comparison of our IRD records with other North Atlantic reconstructions of ice-rafting, sea
484 surface and deep ocean conditions provides a better picture of the development of the LIA. We
485 postulate that the enhanced ice discharge during the MCA, decreased sea surface salinity in the
486 Labrador Sea, which in turn reduced Labrador Sea convection and weakened SPG circulation. The
487 reduction in convection in the Labrador Sea, one of the key areas of deep water formation in the
488 North Atlantic, potentially weakened the AMOC and decreased oceanic heat transport to the high
489 latitudes, particularly to the Labrador Sea region. Reduced convection also diminished the arrival of
490 warm water from the NAC to SE Greenland coasts inducing perennial sea ice occurrence and
491 cooling the atmosphere which and promoted ice sheet growth in the Arctic. Cooling and freshening
492 of the SPG preconditioned the subpolar area to be more sensitive to external forcings. Therefore,
493 the subsequent atmospheric and oceanographic reorganizations induced by solar and volcanic



494 forcing generated extremely cold conditions in the North Atlantic during the LIA, through a shift to
495 predominantly NAO negative conditions and the development of atmospheric blocking events in the
496 North Atlantic. These events boosted further cooling across Europe and the Nordic Seas. The
497 combination of a fresher SPG with the solar-volcanic induced atmospheric change generated harsh
498 conditions in the North Atlantic which caused the abandonment of the Norse colonies in Greenland
499 around 1400 yr AD.

500 This study puts forward the idea that the development of the exceptionally cold conditions of the
501 LIA may be better explained by the previous freshening of the Labrador Sea due to enhanced ice-
502 rafting during the MCA and the subsequent weakening of the SPG circulation. This finding may be
503 fundamental to model future climate conditions given that calving in the SE Greenland glaciers has
504 been increasing during the last decade.

505

506

507 Acknowledgements. This project was funded by NSF grants OCE-0961670 and OCE-1258984, and
508 the Comer Science and Education Foundation grant CP75. Tony Greco is acknowledged for
509 analytical support with the SEM analysis. MAG would like to acknowledge the support from A.E.
510 Shevenell, J. Dixon and D. Hollander during her postdoc at USF, and funding from Portuguese
511 National Science and Technology Foundation (FCT) through the postdoctoral fellowship
512 SFRH/BPD/96960/2013 and CCMAR funding UID/Multi/04326/2013.

513

514

515

516 References

517

518 Alonso-Garcia, M., Andrews, J. T., Belt, S. T., Cabedo-Sanz, P., Darby, D., and Jaeger, J.: A
519 comparison between multiproxy and historical data (AD 1990–1840) of drift ice conditions on the
520 East Greenland shelf (~66°N), *The Holocene*, 23, 1672–1683, 2013.

521 Andresen, C. S., Straneo, F., Ribergaard, M. H., Bjork, A. A., Andersen, T. J., Kuijpers, A.,
522 Norgaard-Pedersen, N., Kjaer, K. H., Schjoth, F., Weckstrom, K., and Ahlstrom, A. P.: Rapid
523 response of Helheim Glacier in Greenland to climate variability over the past century, *Nature*
524 *Geosci*, 5, 37–41, 2012.



- 525 Andrews, J. T., Belt, S. T., Olafsdottir, S., Massé, G., and Vare, L. L.: Sea ice and marine climate
526 variability for NW Iceland/Denmark Strait over the last 2000 cal. yr BP, *The Holocene*, 19, 775-
527 784, 2009a.
- 528 Andrews, J. T., Darby, D., Eberle, D., Jennings, A. E., Moros, M., and Ogilvie, A.: A robust,
529 multisite Holocene history of drift ice off northern Iceland: implications for North Atlantic climate,
530 *The Holocene*, 19, 71-77, 2009b.
- 531 Bailey, I., Foster, G. L., Wilson, P. A., Jovane, L., Storey, C. D., Trueman, C. N., and Becker, J.:
532 Flux and provenance of ice-rafted debris in the earliest Pleistocene sub-polar North Atlantic Ocean
533 comparable to the last glacial maximum, *Earth Planet. Sci. Lett.*, 341–344, 222-233, 2012.
- 534 Bischof, J. F. and Darby, D. A.: Mid- to Late Pleistocene Ice Drift in the Western Arctic Ocean:
535 Evidence for a Different Circulation in the Past, *Science*, 277, 74-78, 1997.
- 536 Blindheim, J. and Malmberg, S. A.: The mean sea level pressure gradient across the Denmark Strait
537 as an indicator of conditions in the North Icelandic Irminger current. In: *The Nordic Seas: An*
538 *Integrated Perspective Oceanography, Climatology, Biogeochemistry, and Modeling*, Geophys.
539 *Monogr. Ser.*, AGU, Washington, DC, 2005.
- 540 Bond, G., Kromer, B., Beer, J., Muscheler, R., Evans, M. N., Showers, W., Hoffmann, S., Lotti-
541 Bond, R., Hajdas, I., and Bonani, G.: Persistent Solar Influence on North Atlantic Climate During
542 the Holocene, *Science*, 294, 2130-2136, 2001.
- 543 Bond, G., Showers, W., Cheseby, M., Lotti, R., Almasi, P., deMenocal, P., Priore, P., Cullen, H.,
544 Hajdas, I., and Bonani, G.: A Pervasive Millennial-Scale Cycle in North Atlantic Holocene and
545 Glacial Climates, *Science*, 278, 1257-1266, 1997.
- 546 Bond, G. C. and Lotti, R.: Iceberg Discharges into the North Atlantic on Millennial Time Scales
547 During the Last Glaciation, *Science*, 267, 1005-1010, 1995.
- 548 Böning, C. W., Scheinert, M., Dengg, J., Biastoch, A., and Funk, A.: Decadal variability of subpolar
549 gyre transport and its reverberation in the North Atlantic overturning, *Geophys. Res. Lett.*, 33,
550 L21S01, doi:10.1029/2006GL026906, 2006.



- 551 Born, A., Nisancioglu, K., and Braconnot, P.: Sea ice induced changes in ocean circulation during
552 the Eemian, *Clim. Dyn.*, 35, 1361-1371, 2010.
- 553 Born, A. and Stocker, T. F.: Two Stable Equilibria of the Atlantic Subpolar Gyre, *J. Phys.*
554 *Oceanogr.*, 44, 246-264, 2014.
- 555 Bradley, R. S., Briffa, K. R., Cole, J., Hughes, M. K., and Osborn, T. J.: The climate of the last
556 millennium. In: *Paleoclimate, global change and the future*, Springer, 2003.
- 557 Copard, K., Colin, C., Henderson, G. M., Scholten, J., Douville, E., Sicre, M. A., and Frank, N.:
558 Late Holocene intermediate water variability in the northeastern Atlantic as recorded by deep-sea
559 corals, *Earth Planet. Sci. Lett.*, 313–314, 34-44, 2012.
- 560 Darby, D. A., Ortiz, J. D., Grosch, C. E., and Lund, S. P.: 1,500-year cycle in the Arctic Oscillation
561 identified in Holocene Arctic sea-ice drift, *Nature Geosci.*, 5, 897-900, 2012.
- 562 Dickson, R. R., Meincke, J., Malmberg, S.-A., and Lee, A. J.: The “great salinity anomaly” in the
563 Northern North Atlantic 1968–1982, *Prog. Oceanogr.*, 20, 103-151, 1988.
- 564 Dickson, R. R., Osborn, T. J., Hurrell, J. W., Meincke, J., Blindheim, J., Adlandsvik, B., Vinje, T.,
565 Alekseev, G., and Maslowski, W.: The Arctic Ocean Response to the North Atlantic Oscillation, *J.*
566 *Clim.*, 13, 2671-2696, 2000.
- 567 Dokken, T. and Ninnemann, U.: Cruise Report R/V G.O. Sars, UoB Cruise No: GS06-144, 2006.
- 568 Fillon, R. H., Miller, G. H., and Andrews, J. T.: Terrigenous sand in Labrador Sea hemipelagic
569 sediments and paleoglacial events on Baffin Island over the last 100, 00 years, *Boreas*, 10, 107-124,
570 1981.
- 571 Gao, C., Robock, A., and Ammann, C.: Volcanic forcing of climate over the past 1500 years: An
572 improved ice core-based index for climate models, *J. Geophys. Res.*, 113, D23111, 2008.
- 573 Grönvold, K., Óskarsson, N., Johnsen, S. J., Clausen, H. B., Hammer, C. U., Bond, G., and Bard,
574 E.: Ash layers from Iceland in the Greenland GRIP ice core correlated with oceanic and land
575 sediments, *Earth Planet. Sci. Lett.*, 135, 149-155, 1995.



- 576 Hakkinen, S. and Rhines, P. B.: Decline of Subpolar North Atlantic Circulation During the 1990s,
577 Science, 304, 555-559, 2004.
- 578 Häkkinen, S., Rhines, P. B., and Worthen, D. L.: Atmospheric blocking and Atlantic multidecadal
579 ocean variability, Science, 334, 655-659, 2011.
- 580 Hatun, H., Sando, A. B., Drange, H., Hansen, B., and Valdimarsson, H.: Influence of the Atlantic
581 Subpolar Gyre on the Thermohaline Circulation, Science, 309, 1841-1844, 2005.
- 582 Henriksen, N., Higgins, A. K., Kalsbeek, F., and Pulvertaft, T. C. R.: Greenland from Archaean to
583 Quaternary. Descriptive text to the 1995 Geological map of Greenland, 1:2 500 000. 2nd edition,
584 Geological Survey of Denmark and Greenland Bulletin, 18, 126 pp + map, 2009.
- 585 Hilmer, M. and Jung, T.: Evidence for a recent change in the link between the North Atlantic
586 Oscillation and Arctic Sea ice export, Geophys. Res. Lett., 27, 989-992, 2000.
- 587 Jennings, A., Thordarson, T., Zalzal, K., Stoner, J., Hayward, C., Geirsdóttir, Á., and Miller, G.:
588 Holocene tephra from Iceland and Alaska in SE Greenland shelf sediments, Geological Society,
589 London, Special Publications, 398, SP398. 396, 2014.
- 590 Jennings, A. E. and Weiner, N. J.: Environmental change in eastern Greenland during the last 1300
591 years: evidence from foraminifera and lithofacies in Nansen Fjord, 68°N, The Holocene, 6, 179-
592 191, 1996.
- 593 Jiang, H., Ren, J., Knudsen, K., Eiríksson, J., and Ran, L.: Summer sea-surface temperatures and
594 climate events on the North Icelandic shelf through the last 3000 years, Chin. Sci. Bull., 52, 789-
595 796, 2007.
- 596 Joughin, I., Howat, I., Alley, R. B., Ekstrom, G., Fahnestock, M., Moon, T., Nettles, M., Truffer,
597 M., and Tsai, V. C.: Ice-front variation and tidewater behavior on Helheim and Kangerdlugssuaq
598 Glaciers, Greenland, Journal of Geophysical Research: Earth Surface, 113, F01004, 2008.
- 599 Kobashi, T., Severinghaus, J., Barnola, J.-M., Kawamura, K., Carter, T., and Nakaegawa, T.:
600 Persistent multi-decadal Greenland temperature fluctuation through the last millennium, Clim.
601 Change, 100, 733-756, 2010.



- 602 Kuijpers, A., Mikkelsen, N., Ribeiro, S., and Seidenkrantz, M.-S.: Impact of medieval fjord
603 hydrography and climate on the western and eastern settlements in Norse Greenland, *Journal of the*
604 *North Atlantic*, 6, 1-13, 2014.
- 605 Lacasse, C.: Influence of climate variability on the atmospheric transport of Icelandic tephra in the
606 subpolar North Atlantic, *Global Planet. Change*, 29, 31-55, 2001.
- 607 Manabe, S. and Stouffer, R. J.: Simulation of abrupt climate change induced by freshwater input to
608 the North Atlantic Ocean, *Nature*, 378, 165-167, 1995.
- 609 Mann, M. E., Zhang, Z., Rutherford, S., Bradley, R. S., Hughes, M. K., Shindell, D., Ammann, C.,
610 Faluvegi, G., and Ni, F.: Global Signatures and Dynamical Origins of the Little Ice Age and
611 Medieval Climate Anomaly, *Science*, 326, 1256-1260, 2009.
- 612 Massé, G., Rowland, S. J., Sicre, M.-A., Jacob, J., Jansen, E., and Belt, S. T.: Abrupt climate
613 changes for Iceland during the last millennium: Evidence from high resolution sea ice
614 reconstructions, *Earth Planet. Sci. Lett.*, 269, 565-569, 2008.
- 615 McManus, J., Major, C., Flower, B., and Fronval, T.: Variability in sea-surface conditions in the
616 North Atlantic-Arctic gateways during the last 140,000 years. In: *Proceedings of the Ocean Drilling*
617 *Program. Scientific results, Volume 151: College Station, TX, Thiede, J., Myhre, A. M., Firth, J. V.,*
618 *Johnson, G. L., and Ruddiman, W. F. (Eds.), Ocean Drilling Program, 1996.*
- 619 Meeker, L. D. and Mayewski, P. A.: A 1400-year high-resolution record of atmospheric circulation
620 over the North Atlantic and Asia, *The Holocene*, 12, 257-266, 2002.
- 621 Miller, G. H., Geirsdóttir, Á., Zhong, Y., Larsen, D. J., Otto-Bliesner, B. L., Holland, M. M.,
622 Bailey, D. A., Refsnider, K. A., Lehman, S. J., Southon, J. R., Anderson, C., Björnsson, H., and
623 Thordarson, T.: Abrupt onset of the Little Ice Age triggered by volcanism and sustained by sea-
624 ice/ocean feedbacks, *Geophys. Res. Lett.*, 39, L02708, 2012.
- 625 Moffa-Sanchez, P., Born, A., Hall, I. R., Thornalley, D. J. R., and Barker, S.: Solar forcing of North
626 Atlantic surface temperature and salinity over the past millennium, *Nature Geosci*, 7, 275-278,
627 2014a.



- 628 Moffa-Sanchez, P., Hall, I. R., Barker, S., Thornalley, D. J. R., and Yashayaev, I.: Surface changes
629 in the eastern Labrador Sea around the onset of the Little Ice Age, *Paleoceanography*, 29,
630 2013PA002523, 2014b.
- 631 Mokeddem, Z. and McManus, J. F.: Persistent climatic and oceanographic oscillations in the
632 subpolar North Atlantic during the MIS 6 glaciation and MIS 5 interglacial, *Paleoceanography*, n/a-
633 n/a, 2016.
- 634 Mokeddem, Z., McManus, J. F., and Oppo, D. W.: Oceanographic dynamics and the end of the last
635 interglacial in the subpolar North Atlantic, *Proceedings of the National Academy of Sciences*, 2014.
- 636 Moreno-Chamarro, E., Zanchettin, D., Lohmann, K., and Jungclauss, J. H.: An abrupt weakening of
637 the subpolar gyre as trigger of Little Ice Age-type episodes, *Clim. Dyn.*, 1-18, 2016.
- 638 Moros, M., Andrews, J. T., Eberl, D. D., and Jansen, E.: Holocene history of drift ice in the
639 northern North Atlantic: Evidence for different spatial and temporal modes, *Paleoceanography*, 21,
640 PA2017, 2006.
- 641 Moros, M., Jansen, E., Oppo, D. W., Giraudeau, J., and Kuijpers, A.: Reconstruction of the late-
642 Holocene changes in the Sub-Arctic Front position at the Reykjanes Ridge, north Atlantic, *The*
643 *Holocene*, 22, 877-886, 2012.
- 644 Moros, M., McManus, J. F., Rasmussen, T., Kuijpers, A., Dokken, T., Snowball, I., Nielsen, T., and
645 Jansen, E.: Quartz content and the quartz-to-plagioclase ratio determined by X-ray diffraction: a
646 proxy for ice rafting in the northern North Atlantic?, *Earth Planet. Sci. Lett.*, 218, 389-401, 2004.
- 647 Mugford, R. I. and Dowdeswell, J. A.: Modeling iceberg-rafted sedimentation in high-latitude fjord
648 environments, *Journal of Geophysical Research: Earth Surface*, 115, F03024, 2010.
- 649 Murray, T., Scharrer, K., James, T. D., Dye, S. R., Hanna, E., Booth, A. D., Selmes, N., Luckman,
650 A., Hughes, A. L. C., Cook, S., and Huybrechts, P.: Ocean regulation hypothesis for glacier
651 dynamics in southeast Greenland and implications for ice sheet mass changes, *Journal of*
652 *Geophysical Research: Earth Surface*, 115, F03026, 2010.
- 653 Mysak, L. A.: Patterns of Arctic Circulation, *Science*, 293, 1269-1270, 2001.



- 654 Nyland, B. F., Jansen, E., Elderfield, H., and Andersson, C.: Neogloboquadrina pachyderma (dex.
655 and sin.) Mg/Ca and d18O records from the Norwegian Sea, *Geochem. Geophys. Geosyst.*, 7,
656 Q10P17, doi:10.1029/2005GC001055, 2006.
- 657 Ogilvie, A. E. J., Barlow, L. K., and Jennings, A. E.: North Atlantic climate c.ad 1000: Millennial
658 reflections on the Viking discoveries of Iceland, Greenland and North America, *Weather*, 55, 34-45,
659 2000.
- 660 Ogilvie, A. E. J. and Jónsson, T.: "Little Ice Age" Research: A Perspective from Iceland, *Clim.
661 Change*, 48, 9-52, 2001.
- 662 Olsen, J., Anderson, N. J., and Knudsen, M. F.: Variability of the North Atlantic Oscillation over
663 the past 5,200 years, *Nature Geosci*, 5, 808-812, 2012.
- 664 PAGES 2k Consortium: Continental-scale temperature variability during the past two millennia,
665 *Nature Geosci*, 6, 339-346, 2013.
- 666 Petersen, H. I., Øverland, J. A., Solbakk, T., Bojesen-Koefoed, J. A., and Bjerager, M.: Unusual
667 resinite-rich coals found in northeastern Greenland and along the Norwegian coast: Petrographic
668 and geochemical composition, *Int. J. Coal Geol.*, 109-110, 58-76, 2013.
- 669 Reeh, N., Thomsen, H. H., Higgins, A. K., and Weidick, A.: Sea ice and the stability of north and
670 northeast Greenland floating glaciers, *Ann. Glaciol.*, 33, 474-480, 2001.
- 671 Rhein, M., Fischer, J., Smethie, W., Smythe-Wright, D., Weiss, R., Mertens, C., Min, D.-H.,
672 Fleischmann, U., and Putzka, A.: Labrador Sea Water: Pathways, CFC inventory, and formation
673 rates, *J. Phys. Oceanogr.*, 32, 648-665, 2002.
- 674 Rignot, E. and Kanagaratnam, P.: Changes in the Velocity Structure of the Greenland Ice Sheet,
675 *Science*, 311, 986-990, 2006.
- 676 Rigor, I. G., Wallace, J. M., and Colony, R. L.: Response of Sea Ice to the Arctic Oscillation, *J.
677 Clim.*, 15, 2648-2663, 2002.



- 678 Ruddiman, W. F.: Late Quaternary deposition of ice rafted sand in the subpolar North Atlantic (lat
679 40° to 65° N), Geol. Soc. Am. Bull., 88, 1813-1827, 1977.
- 680 Sarafanov, A.: On the effect of the North Atlantic Oscillation on temperature and salinity of the
681 subpolar North Atlantic intermediate and deep waters, ICES Journal of Marine Science: Journal du
682 Conseil, 66, 1448-1454, 2009.
- 683 Schmitz, W. J. and McCartney, M.: On the North Atlantic Circulation, Rev. Geophys., 31, 29-49,
684 1993.
- 685 Sejrup, H. P., Lehman, S. J., Hafliðason, H., Noone, D., Muscheler, R., Berstad, I. M., and
686 Andrews, J. T.: Response of Norwegian Sea temperature to solar forcing since 1000 A.D, J.
687 Geophys. Res., 115, C12034, 2010.
- 688 Shabbar, A., Huang, J., and Higuchi, K.: The relationship between the wintertime North Atlantic
689 Oscillation and blocking episodes in the North Atlantic, Int. J. Climatol., 21, 355-369, 2001.
- 690 Sicre, M.-A., Jacob, J., Ezat, U., Rousse, S., Kissel, C., Yiou, P., Eiríksson, J., Knudsen, K. L.,
691 Jansen, E., and Turon, J.-L.: Decadal variability of sea surface temperatures off North Iceland over
692 the last 2000 years, Earth Planet. Sci. Lett., 268, 137-142, 2008.
- 693 Sicre, M. A., Weckström, K., Seidenkrantz, M. S., Kuijpers, A., Benetti, M., Masse, G., Ezat, U.,
694 Schmidt, S., Bouloubassi, I., Olsen, J., Khodri, M., and Mignot, J.: Labrador current variability over
695 the last 2000 years, Earth Planet. Sci. Lett., 400, 26-32, 2014.
- 696 Steinhilber, F., Beer, J., and Fröhlich, C.: Total solar irradiance during the Holocene, Geophys. Res.
697 Lett., 36, L19704, doi:19710.11029/12009GL040142, 2009.
- 698 Talley, L. D.: Shallow, intermediate, and deep overturning components of the global heat budget, J.
699 Phys. Oceanogr., 33, 530-560, 2003.
- 700 Thornalley, D. J. R., Elderfield, H., and McCave, I. N.: Holocene oscillations in temperature and
701 salinity of the surface subpolar North Atlantic, Nature, 457, 711-714, 2009.



702 Trouet, V., Esper, J., Graham, N. E., Baker, A., Scourse, J. D., and Frank, D. C.: Persistent Positive
703 North Atlantic Oscillation Mode Dominated the Medieval Climate Anomaly, *Science*, 324, 78-80,
704 2009.

705 Wanner, H., Mercolli, L., Grosjean, M., and Ritz, S. P.: Holocene climate variability and change; a
706 data-based review, *J. Geol. Soc.*, 172, 254-263, 2015.

707 Wanner, H., Solomina, O., Grosjean, M., Ritz, S. P., and Jetel, M.: Structure and origin of Holocene
708 cold events, *Quat. Sci. Rev.*, 30, 3109-3123, 2011.

709 Yang, Q., Dixon, T. H., Myers, P. G., Bonin, J., Chambers, D., and van den Broeke, M. R.: Recent
710 increases in Arctic freshwater flux affects Labrador Sea convection and Atlantic overturning
711 circulation, *Nat Commun*, 7, 2016.

712

713

714

715

716

717

718

719

720

721

722

723

724

725

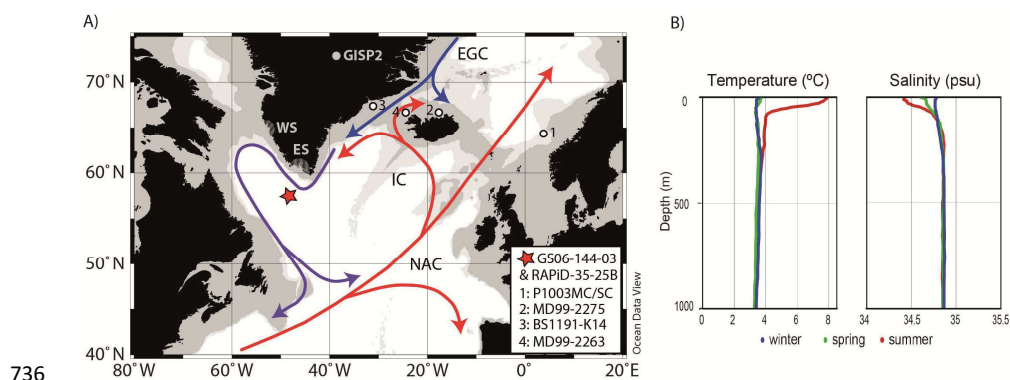
726

727



728 Figure Captions

729 Figure 1. A) Location of multicore GS06-144-03 (red star) and other sites in the Northern North
730 Atlantic whose records have been used to support the hypothesis proposed in this work. General
731 North Atlantic circulation is shown according to Schmitz and McCartney (1993). The location of
732 Norse settlements in Greenland is shaded and indicated with ES (Eastern settlement) and WS
733 (Western settlement). B) Temperature and salinity profiles of the first 1000 m at site GS06-144-03
734 obtained through Ocean Data View (<http://odv.awi.de/en/home/>) from the World Ocean Atlas 2013
735 (Locarnini et al., 2013; Zweng et al., 2013).

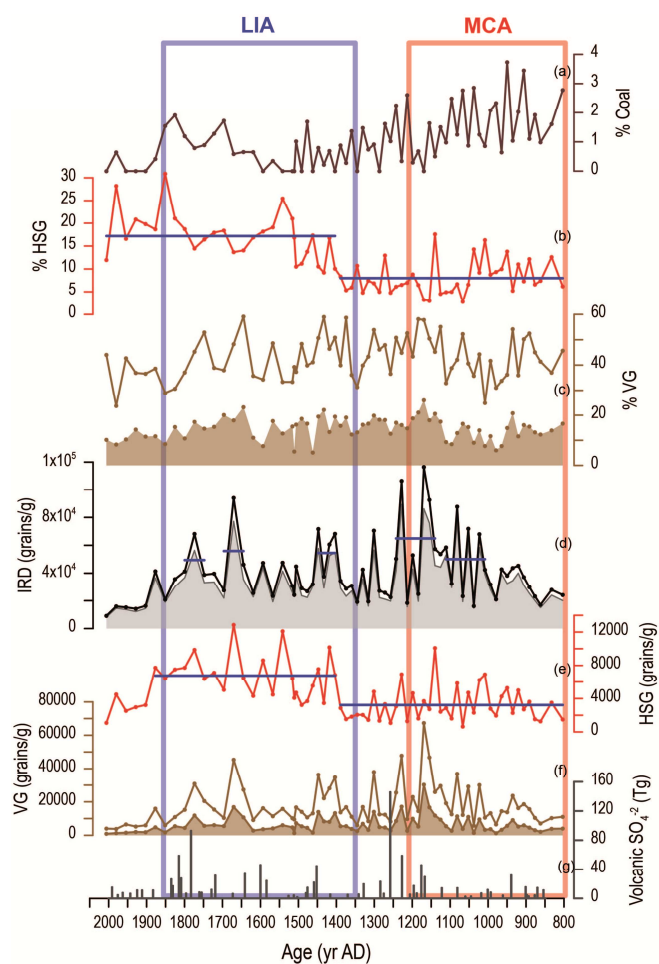


736

737



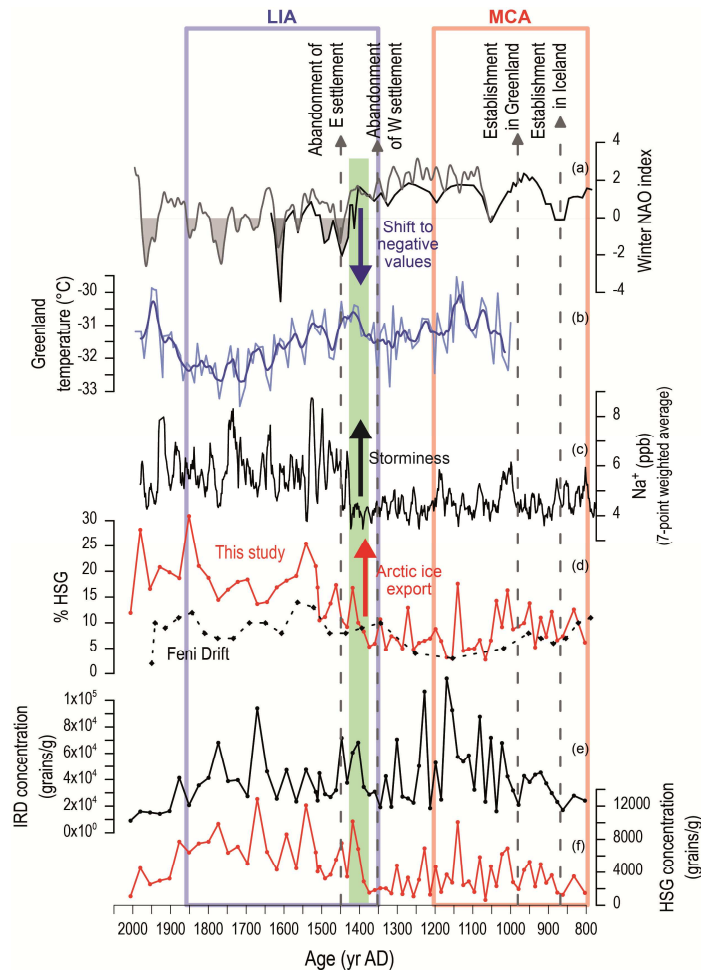
738 Figure 2. Ice-rafted debris (IRD) records from site GS06-144-03. a) Coal grains relative abundance;
739 b) Hematite stained grains (HSG) relative abundance; c) total volcanic glass (VG) relative
740 abundance (brown line) and white VG relative abundance (shaded area); d) total IRD concentration
741 in each sediment sample (black line), and IRD concentration not including the white volcanic glass
742 (shaded area); e) concentration of HSG; f) concentration of total VG (brown line) and white VG
743 (shaded area); g) Northern Hemisphere sulphate aerosol injection by volcanic eruptions (after Gao
744 et al. (2008), revised in 2012). Blue horizontal lines indicate mean values for the intervals they
745 encompass. The approximate standard duration of the Little Ice Age (LIA) and Medieval Warm
746 Period (MWP) has been shaded in blue and red respectively.



747



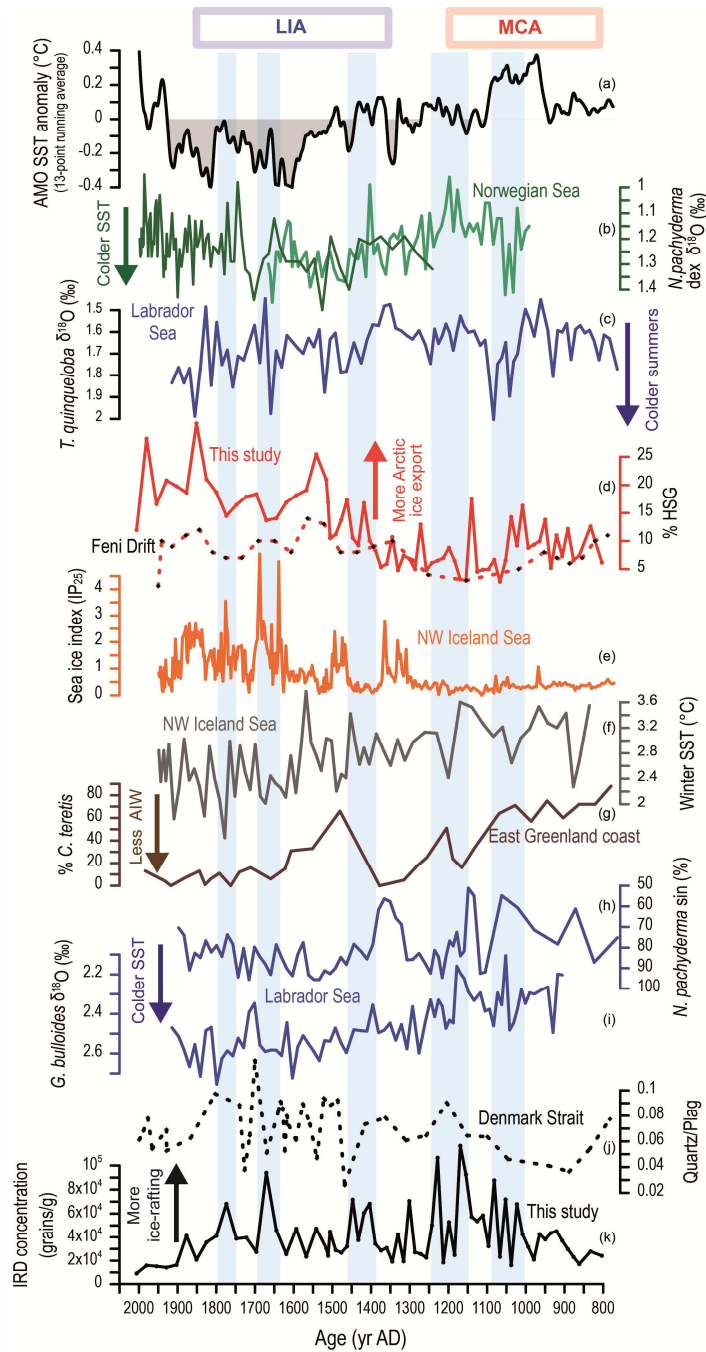
748 Figure 3. LIA shift at ~1400 yr AD (green vertical bar) in several records compared to site GS06-
 749 144-03 IRD records. a) Winter NAO index reconstructions by Trouet et al. (2009, grey line) and
 750 Olsen et al. (2012, black line); b) Greenland surface temperature reconstruction of the last
 751 millennium (Kobashi et al., 2010); c) Na⁺ record from GISP2 (Meeker and Mayewski, 2002); d)
 752 HSG record from Eirik Drift (red line) and from Feni Drift in the NE Atlantic (black dashed line,
 753 Bond et al., 2001); e) total IRD concentration; f) HSG concentration. The main events in Norse
 754 colonisation and abandonment of settlements are depicted on the top of the figure, according to
 755 Ogilvie et al. (2000).



756



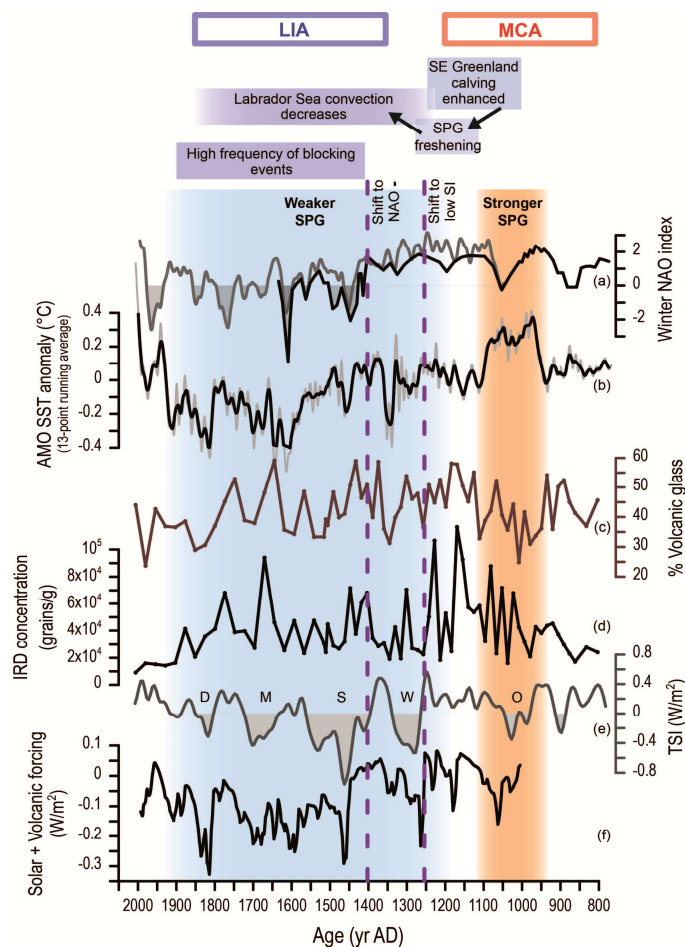
757 Figure 4. Comparison of IRD records from site GS06-144-03 with subpolar North Atlantic records
758 of sea surface temperature, ice-rafting and sea ice. a) Atlantic Multidecadal Oscillation (AMO) SST
759 anomaly (Mann et al., 2009); b) *N. pachyderma* $\delta^{18}\text{O}$ record from the Norwegian Sea (Sejrup
760 et al., 2010), c) *T. quinqueloba* $\delta^{18}\text{O}$ record from site RAPiD-35-25B at Eirik Drift; d) HSG
761 relative abundance from site GS06-144-03 (solid line, this study) and from Feni Drift (dashed line,
762 Bond et al., 2001), e) Sea ice index (IP25) from site MD99-2275, NW of Iceland (Massé et al.,
763 2008), f) Diatom-based winter SST from site MD99-2275 (Jiang et al., 2007), g) Relative
764 abundance of the Atlantic waters indicator *Cassidulina teretis* from Nansen Fjord (Jennings and
765 Weiner, 1996), h) Relative abundance of *N. pachyderma* *sin* from Eirik Drift (Moffa-Sanchez et al.,
766 2014b), i) *G. bulloides* $\delta^{18}\text{O}$ from Eirik Drift (Moffa-Sanchez et al., 2014a), j) Quartz vs
767 plagioclase ratio, a proxy for ice-rafting, from MD99-2263 (Andrews et al., 2009), k) total IRD
768 concentration from site GS06-144-03 (this study). Grey vertical bars indicate the periods in which
769 IRD concentration is higher at site GS06-144-03.



770



771 Figure 5. Sequence of events during the transition from the MCA to LIA and correlation to the
 772 potential forcings. a) Winter NAO index reconstructions by Trouet et al. (2009, grey line) and Olsen
 773 et al. (2012, black line); b) Atlantic Multidecadal Oscillation (AMO) SST anomaly (Mann et al.,
 774 2009); c) total volcanic glass (VG) relative abundance at site GS06-144-03 ; d) total IRD
 775 concentration at site GS06-144-03; e) Reconstruction of total solar irradiance based on 10Be
 776 isotopes from ice cores (Steinhilber et al., 2009); f) Net radiative forcing based on solar irradiance
 777 and volcanic eruption reconstructions (Crowley, 2000). During the interval shaded in red SPG
 778 circulation was stronger, according to the interpretations of this work, whereas during the interval
 779 shaded in blue SPG circulation was weak. The letters in the solar irradiance record indicate the
 780 minima of solar irradiance named Oort (O), Wolf (W), Spörer (S), Maunder (M) and Dalton (D).



781